This is a preprint, the final version is subject to change, of the American Mineralogist (MSA)
Cite as Authors (Year) Title. American Mineralogist, in press.
DOI: https://doi.org/10.2138/am-2019-6925

Ascent of water-rich magma and decompression heating: a thermodynamic analysis

ALLEN F. GLAZNER

Department of Geological Sciences, University of North Carolina, Chapel Hill, North Carolina 27599-3315, U.S.A.

ABSTRACT

Ascent of hydrous, silica-rich magmas from the lower crust drives volcanic eruptions, builds the upper crust, and concentrates metals such as Cu, Au, and Mo into ore deposits. Owing to the negative slope of the melting curve for granitic materials in the presence of water, it has long been assumed that water-saturated magmas move into the subsolidus field and freeze upon ascent; therefore, for a magma to rise it must be water-undersaturated at a temperature well above the solidus. This assumption ignores the considerable energy released by crystallization. Here I show that if magma ascent is treated as an adiabatic, reversible process then water-saturated magma can rise to the surface, following the solidus to shallow depth and higher temperature as it undergoes modest crystallization and vapor exsolution. Decompression heating is an alternative to magma recharge for explaining pre-eruptive reheating seen in many volcanic systems and accounts for paradoxical growth of quartz during a heating event. The viscosity increase that accompanies vapor exsolution as magma rises to shallow depth explains why silicic magmas tend to stop in the upper crust rather than erupting, producing the observed compositional dichotomy between plutonic and volcanic rocks.

keywords: thermodynamics, magma, decompression, adiabatic, granite, rhyolite

Always consult and cite the final, published document. See http:/www.minsocam.org or GeoscienceWorld

This is a preprint, the final version is subject to change, of the American Mineralogist (MSA)
Cite as Authors (Year) Title. American Mineralogist, in press.
DOI: https://doi.org/10.2138/am-2019-6925

INTRODUCTION

Abundant silicic magmatism distinguishes the Earth from other bodies in the solar system, and Earth's continents were built largely by distilling silicic and intermediate magmas from the mantle in subduction systems. Silicic magmas can be produced from basaltic magma by crystal-liquid separation (Bowen 1915), or by partial melting of a wide variety of crustal materials including silicate-rich igneous and metamorphic rocks (Clemens and Wall 1981; Brown 1994; Patiño-Douce and Beard 1995) and hydrous mafic rocks such as amphibolite (Beard and Lofgren 1991; Sisson et al. 2005), with water playing a key role in both promoting melting and controlling the composition of the resulting melt.

The continental crust is chemically stratified, with relatively high-SiO_2 rocks concentrated in the upper crust (average 67 wt% SiO_2; Rudnick and Gao 2013). These estimates are consistent with exposed sections of arc crust (Jagoutz and Kelemen 2015), and the shallow crust exposed in many extinct arcs contains great volumes of relatively high-SiO_2 granites and granodiorites (Fig. 2) that were emplaced at upper-crustal depths (Hamilton and Myers 1967; Myers 1975; Ague and Brimhall 1988; Singh et al. 2007; Bagdonas et al. 2016). Although plutons emplaced at greater depths are common worldwide, the dominant granites, granodiorites, and tonalites in many arcs were emplaced at depths of <15 km.

Tuttle and Bowen (1958) showed that partial melting and fractional crystallization in the granite system albite-orthoclase-quartz-H_2O produce eutectic high-silica rhyolitic compositions that match granites found in nature, and this work led to acceptance of granites as fundamentally igneous. They also showed that the solidus is dramatically depressed in the presence of water under pressure, falling some 300 °C as pressure increases from one atmosphere to 400 MPa (Fig. 2). This was in turn interpreted to mean that, owing to the negative slope of the water-saturated solidus, a melt parcel rising from the solidus along a near-isothermal path will freeze as it moves

Always consult and cite the final, published document. See http:/www.minsocam.org or GeoscienceWorld

into the subsolidus field (Cann 1970; Harris et al. 1970; Fig. 2, path A-B), preventing water-saturated rhyolitic magmas from ascending.

This hypothesis provided a simple explanation for the longstanding observation that low-SiO_2 rocks seem to predominate among volcanic rocks whereas granites predominate among shallow intrusive rocks (Daly 1914). Compilations of chemical analyses from various continental geologic provinces (Fig. 2) bear this out; volcanic rocks tend to have a mode in the andesite range, whereas plutonic rocks tend to have a mode in the granite range, ~70 wt% SiO_2. These compilations are clearly subject to collection bias, exposure bias, and other sources of uncertainty, but the pattern of silicic compositions dominating plutonic rocks and more mafic compositions dominating volcanic rocks is widespread.

The supposed inability of water-saturated silicic magmas to rise led to a conundrum: there is little evidence for generation of granitic magmas in the upper crust, because the residues of such a process (e.g., partially melted crustal rocks or the mafic complements of fractional crystallization) are rarely found there; thus, how do such magmas rise from deeper sources to their emplacement levels? The explanation generally offered is that the magmas form by dehydration melting at temperatures well above the solidus (Clemens 1984; Johannes and Holtz 1996), or are heated to such temperatures. Such magmas are significantly water-undersaturated, allowing them to avoid crystallization along approximately isothermal ascent paths until they hit the solidus at shallow depth (Fig. 2, path D-E).

Ascent of hydrous, silica-rich magma from deeper parts of the crust drives a number of important geologic processes, including volcanic eruptions (Blundy and Cashman 2001; Waters and Lange 2017), supereruptions (Miller and Wark 2008), pluton emplacement (Annen et al. 2006; Schoene et al. 2012), and formation of ore deposits (Rosera et al. 2013; Mercer et al. 2015). The assumption that water-saturated high-silica magmas that lie near the solidus cannot

Always consult and cite the final, published document. See http:/www.minsocam.org or GeoscienceWorld

This is a preprint, the final version is subject to change, of the American Mineralogist (MSA)
Cite as Authors (Year) Title. American Mineralogist, in press.
DOI: https://doi.org/10.2138/am-2019-6925

rise owing to the negative slope of the solidus is generally built into these analyses (e.g., Müller et al. 2010; Collins et al. 2016). However, as I demonstrate below, this assumption is incorrect.

The argument that a melt parcel rising isothermally from the solidus will immediately freeze is correct, but relies on the incorrect assumption that an adiabatic ascent path in a crystal-liquid system will be approximately isothermal, similar to that of a rising parcel of unmelted mantle under a mid-ocean ridge (McKenzie and Bickle 1988). Tuttle and Bowen (1958) recognized that such a path is not likely because it requires extracting a significant quantity of latent heat of fusion, a point that has been largely forgotten. An estimate of the magnitude of the problem is given by dividing the latent heat of fusion (J kg^{-1}) of a relevant phase, such as albite (Lange and Carmichael 1990), by its heat capacity (J kg^{-1} K^{-1}); the result, ~200 °K, is how much this latent heat could raise the temperature of an equivalent mass of albite crystals. Blundy et al. (2006) showed that various eruptive products of Mount St. Helens and Shiveluch volcanoes record evidence for up to 100 °C of heating during ascent, and attributed this to release of latent heat of fusion during decompression and loss of dissolved water.

In this paper I develop a thermodynamic analysis of adiabatic ascent of hydrous high-silica melt. Such melt rising from the solidus will not freeze but instead will follow the solidus to shallow depth, rising in temperature by 100 °C or more (Fig. 2, path A-F), consistent with the data of Blundy et al. (2006). The formal analysis uses the system albite-H_2O, for which abundant thermodynamic data exist, but the principles developed should be equally applicable to the granite minimum-melt system and to the genesis of high-silica rhyolites.

METHODS

All calculations were made relative to a standard state T_0, P_0 of 0 °C and 10^5 Pa, in specific (per gram) units, using data from Burnham et al. (1969), Burnham and Davis (1971,

Always consult and cite the final, published document. See http:/www.minsocam.org or GeoscienceWorld

This is a preprint, the final version is subject to change, of the American Mineralogist (MSA)
Cite as Authors (Year) Title. American Mineralogist, in press.
DOI: https://doi.org/10.2138/am-2019-6925

1974), Robie et al. (1978), and Tribaudino et al. (2010). The temperature and pressure derivatives of entropy are

$$\left(\frac{\partial S}{\partial T}\right)_P = \frac{C_P}{T} \quad (1)$$

$$\left(\frac{\partial S}{\partial P}\right)_T = -\alpha v \quad (2)$$

where C_p is the heat capacity function, α is the thermal expansion coefficient defined by

$$\alpha = \frac{1}{V}\frac{dV}{dT} \quad (3)$$

and v is the molar volume (Lewis et al. 1961). The specific entropy of crystalline albite at *P* and *T* was calculated by

$$S_{ab}^{P,T} = \int_{T_0}^{T} \frac{C_p}{T} dT + \int_{P_0}^{P} (-\alpha v) dP \quad (4)$$

The pressure term is insignificant.

The partial molal entropies of the two melt components were calculated using the method of Burnham and Davis (1974), who chose H_2O and $NaAlSi_3O_8$ as molar mixing components. The partial molal entropy of albite $\overline{S}_{ab}^{m}$ in hydrous melt was determined by calculating the entropy of albite glass at *T* and 10^5 Pa by integrating C_p / T for albite glass as above and then adding in pressure and composition terms relative to the glass standard state at *T* and 10^5 Pa from equation 45 of Burnham and Davis (1974). The partial molal entropy of water $\overline{S}_{w}^{m}$ in hydrous melt was calculated by adding values from their Figure 15 at values of *P* and *T* along the solidus using the graphical solution in their Figures 15 and 16; the difference in pressure solid state between their value (water triple point) and 10^5 Pa is negligible and was ignored. The specific entropy of the hydrous melt was then calculated by combining the partial molal quantities:

Always consult and cite the final, published document. See http:/www.minsocam.org or GeoscienceWorld

This is a preprint, the final version is subject to change, of the American Mineralogist (MSA)
Cite as Authors (Year) Title. American Mineralogist, in press.
DOI: https://doi.org/10.2138/am-2019-6925

$$s_m = X_w \overline{s}_w + X_{ab} \overline{s}_{ab} \quad (5)$$

where s_m is the specific entropy of the hydrous melt, $\overline{s}_w$ and $\overline{s}_{ab}$ are the partial molal entropies of the water and albite components in the melt, and X_w and X_{ab} are their mole fractions, calculated using H_2O and $NaAlSi_3O_8$ as components.

The specific entropy of the vapor phase was taken to be equal to that of pure water (Burnham et al. 1969) because the location and shape of the vaporus (melt-vapor boundary) in Figure 3 are speculative. Assuming a likely vapor composition (e.g., weight fraction = 0.9, which is a mole fraction of 0.99) and using partial molal values as above yields somewhat different values, but the points for different pressures move together and the effect on calculated phase proportions is small.

ADIABATIC ASCENT AND DECOMPRESSION HEATING

McKenzie and Bickle (1988) estimated the temperature change accompanying adiabatic ascent of mantle peridotite using

$$\left(\frac{\partial T}{\partial z}\right)_S = \frac{g\alpha T}{C_p} \quad (5)$$

where T is temperature, z is depth (increasing downward), g is the acceleration due to gravity, α is the thermal expansion coefficient of the melt, and C_p is the heat capacity at constant pressure. They calculated that a parcel of rising peridotite should cool at ~1 °C/km for typical values of the right-side parameters. This relatively small gradient means that adiabatic ascent paths for such systems are steep on *P-T* diagrams.

Equation 5 only applies to systems that are not undergoing phase changes, a special case of adiabatic ascent. Following methods used to study decompression melting of the mantle (Asimow 2000; Ganguly 2005) or ascent of moist air in the atmosphere (Pruppacher and Klett

Always consult and cite the final, published document. See http:/www.minsocam.org or GeoscienceWorld

This is a preprint, the final version is subject to change, of the American Mineralogist (MSA)
Cite as Authors (Year) Title. American Mineralogist, in press.
DOI: https://doi.org/10.2138/am-2019-6925

2010), adiabatic ascent of magma with phase changes can be idealized as a reversible adiabatic process. Although adiabatic processes are commonly equated with isenthalpic processes (Waldbaum 1971; Blundy et al. 2006), this is not the case for a system moving in a gravitational field (Ramberg 1971). For a reversible adiabatic process $dS = \frac{\delta q_{rev}}{T}$ where *S*, *q*, and *T* are entropy, heat, and temperature, and δq_{rev} is an infinitesimal amount of heat transferred along a given thermodynamic path. For an adiabatic process $\delta q_{rev} = 0$ and thus the entropy change is zero (Lewis et al. 1961); the process is isentropic as long as there is no irreversible entropy production, as by shear heating or mixing (Asimow 2000). Thus, entropy will be conserved (constant) in a parcel of melt rising from its source region adiabatically and reversibly.

Here I calculate the entropies of albite melt, crystals, and vapor and track changes in these three phases during ascent. Calculating the entropies of crystals and water vapor relative to a given standard state is readily done with available data, but the entropy of silicate melts is generally poorly known. However, experimental work (Burnham et al. 1969; Burnham and Davis 1974; Robie et al. 1978; Tribaudino et al. 2010) provides extensive thermodynamic data for the system albite-H_2O (Fig. 3), which has long been used as a model for the granite system.

Consider the water-present solidus in the system albite-H_2O at 800 MPa, 738 °C (white star, Fig. 3a). Along this curve three phases coexist: albite (**a**), hydrous melt (**m**), and H_2O-rich vapor (**v**) (Fig. 3b). All share the same values of the intensive variables pressure *P* and temperature *T*, but have different specific entropies *s*. On a plot of *s* vs. *P* these phases form a three-phase triangle (Figs. 3c, 4), just as the eutectic in a standard temperature-composition (*T*-*X*) binary phase diagram expands to a triangle when recast as an enthalpy-composition (*H*-*X*) diagram (Ussler and Glazner 1992; Glazner 2007).

Always consult and cite the final, published document. See http:/www.minsocam.org or GeoscienceWorld

This is a preprint, the final version is subject to change, of the American Mineralogist (MSA)
Cite as Authors (Year) Title. American Mineralogist, in press.
DOI: https://doi.org/10.2138/am-2019-6925

If a parcel of melt (star in Fig. 4) separates from the **a-m-v** assemblage and rises to lower *P*, then the resulting assemblage remains at the same *s* and weight fraction H_2O. Triangles for lower pressures are shown in Figure 4, and they enclose the 800 MPa melt point; for an 800 MPa melt parcel rising adiabatically and isentropically the proportions of **a**, **m**, and **v** can be calculated using the lever rule. These calculations show, for example, that a parcel consisting of 100% melt, rising from 800 MPa (~30 km depth) to 200 MPa (~8 km), will crystallize to 29 wt% **a**, 62 wt% **m**, and 9 wt% **v** at 832 °C, undergoing nearly 100 °C of decompression heating. The three-phase assemblage slides down the solidus to lower *P* and higher *T*, partially crystallizing and exsolving vapor. As noted by Tuttle and Bowen (1958), the system paradoxically crystallizes partially even though its temperature rises. I do not extrapolate below 100 MPa owing to a lack of data, but it seems clear that such a parcel could theoretically make it to the surface without fully crystallizing. The same general history would be followed by a mixture of **m**+**v** (melt + vapor bubbles).

A water-undersaturated melt produced at a temperature above the solidus lies on the **a**-**m** curve (e.g., red stars in Fig. 3). If it rises isentropically the triangles of Figure 4 grow with decreasing *P* to eventually enclose it at ~300 MPa, where it becomes water-saturated and hits the solidus (=liquidus). It will then travel down the solidus and up in *T* with decreasing *P* as in the water-saturated case. In these calculations **m** lies very close to the **a**-**m** curve as *P* decreases, essentially following the water-undersaturated liquidus (in this case at a weight fraction of water between 0.07 and 0.08) at decreasing *T* until it hits the solidus (Fig. 3a). An equivalent path in the granite system is shown schematically by Figure 2, path D-C-F.

STALLING IN THE SHALLOW CRUST

These calculations show that a melt parcel rising from either the water-saturated solidus or from water-undersaturated conditions at higher *T* can rise without fully crystallizing, and yet

Always consult and cite the final, published document. See http:/www.minsocam.org or GeoscienceWorld

This is a preprint, the final version is subject to change, of the American Mineralogist (MSA)
Cite as Authors (Year) Title. American Mineralogist, in press.
DOI: https://doi.org/10.2138/am-2019-6925

the geologic record clearly shows that a significant fraction of silicic magmas end up crystallizing in the upper crust rather than erupting. A likely explanation for why these magmas stall in the shallow crust is the increase in viscosity that accompanies such ascent. As noted by Blundy et al. (2006), in the granite-H_2O system (Fig. 2), the viscosity of melt rising along the solidus depends on the competition between increasing *T* and loss of water, because the water content at saturation decreases with decreasing *P* and thus with increasing *T*. A rough estimate of these effects is shown in Figure 5, which plots melt viscosity (Giordano et al. 2008) for minimum-melt granite along the solidus as a function of pressure; viscosity rises from 10^3 Pa·s at 800 MPa to 10^6 Pa·s at 100 MPa, and adding in the effect of crystals increases the viscosity at lower *P* by a factor of 10 to 100 depending on the rheologic model used.

Water-rich granitic magma with a viscosity of 10^4-10^5 Pa·s is generally considered capable of rapid ascent in dikes (Clemens and Mawer 1992; Petford et al. 2000). However, at *P* <200 MPa a rising parcel of magma will undergo a super-exponential increase in viscosity, reaching values comparable to those estimated for the extremely viscous Mount St. Helens dome (Pinkerton and Stevenson 1992). This poses a significant barrier to further ascent, and this increase in viscosity in spite of decompression heating is likely why many silicic magmas freeze into plutons before erupting. Recharge (Wark et al. 2007; Shane et al. 2008; Singer et al. 2016) and other dynamic events may help a magma through this barrier to produce an eruption, and kinetic delays in nucleation of super-liquidus magmas (Waters et al. 2015) can suppress the viscosity increase caused by crystallization, further aiding ascent.

DECOMPRESSION HEATING AND PRE-ERUPTIVE EVENTS

Decompression heating of water-rich magma during ascent offers an alternative to recharge by hotter magma to explain late-stage thermal events in silicic magmas. Quartz crystals in a number of rhyolites and granites have Ti-rich rims that suggest late-stage temperature

Always consult and cite the final, published document. See http:/www.minsocam.org or GeoscienceWorld

This is a preprint, the final version is subject to change, of the American Mineralogist (MSA)
Cite as Authors (Year) Title. American Mineralogist, in press.
DOI: https://doi.org/10.2138/am-2019-6925

increases of 50 °C or more (Wark et al. 2007). These are typically explained as recharge events, and paradoxical growth of quartz during *T* increases is usually attributed to simultaneous lowering of the activity of water in the melt by introduction of CO_2. However, Thomas and Watson (2012) showed that lowering *P* at constant *T* will also increase the Ti concentration in quartz. They argued that the observed rimward Ti increases can be generated by decompression along an isothermal path (Fig. 6). Decompression heating offers a third option, in which magma generated at higher *P* slides along the solidus to lower *P* and higher *T*, and crystal growth occurs during decompression heating without requiring a simultaneous lowering of water activity.

IMPLICATIONS FOR SILICIC MAGMATISM

The longstanding assumptions that (1) water-saturated silicic magmas ascending adiabatically will freeze at the solidus; (2) water-undersaturated magmas will freeze upon adiabatic ascent to the solidus; and (3) adiabatic ascent of melt-crystal mixtures is nearly isothermal, are invalid. Assuming that magma ascent can be idealized as a reversible adiabatic (isentropic) process, entropy calculations demonstrate that such magmas will follow the solidus as they ascend, rising in temperature while they partially crystallize and exsolve water-rich vapor. This means that the solidus does not act as a barrier to ascent of water-rich magmas but instead serves as a pathway to the surface in *P*-*T* space. However, silicic melt rising by any mechanism must exsolve water vapor as it rises, causing a significant increase in viscosity; coupled with decompression crystallization (Blundy and Cashman 2001), this viscosity increase is likely an important reason that silicic magmas are likely to get stuck in the upper crust rather than to erupt, leading to the observed predominance of silicic plutons in the upper crust and mafic and intermediate lavas on the surface.

Always consult and cite the final, published document. See http:/www.minsocam.org or GeoscienceWorld

This is a preprint, the final version is subject to change, of the American Mineralogist (MSA)
Cite as Authors (Year) Title. American Mineralogist, in press.
DOI: https://doi.org/10.2138/am-2019-6925

ACKNOWLEDGMENTS

This work was inspired by discussions held at a Royal Society meeting on magma reservoirs in November 2017. Careful pre-review by Bill Ussler and Lang Farmer greatly improved the logic and presentation, as did excellent journal reviews by Kelly Russell and Luca Caricchi. This work was supported by the Mary Lily Kenan Flagler Bingham Professorship.

REFERENCES

Ague, J.J., and Brimhall, G.H. (1988) Magmatic arc asymmetry and distribution of anomalous plutonic belts in the batholiths of California; effects of assimilation, crustal thickness, and depth of crystallization. Geological Society of America Bulletin, 100, 912–927.

Annen, C., Scaillet, B., and Sparks, R.S.J. (2006) Thermal constraints on the emplacement rate of a large intrusive complex; the Manaslu Leucogranite, Nepal Himalaya. Journal of Petrology, 47, 71–95.

Asimow, P.D. (2000) Melting the mantle. In H. Sigurdsson, Ed., Encyclopedia of Volcanoes pp. 55–68. Academic Press, San Diego.

Bagdonas, D.A., Frost, C.D., and Fanning, C.M. (2016) The origin of extensive Neoarchean high-silica batholiths and the nature of intrusive complements to silicic ignimbrites: Insights from the Wyoming batholith, U.S.A. American Mineralogist, 101, 1332–1347.

Beard, J.S., and Lofgren, G.E. (1991) Dehydration melting and water-saturated melting of basaltic and andesitic greenstones and amphibolites at 1, 3, and 6.9 kb. Journal of Petrology, 32, 365–401.

Blundy, J., and Cashman, K. (2001) Ascent-driven crystallisation of dacite magmas at Mount St. Helens, 1980-1986. Contributions to Mineralogy and Petrology, 140, 631–650.

Always consult and cite the final, published document. See http:/www.minsocam.org or GeoscienceWorld

This is a preprint, the final version is subject to change, of the American Mineralogist (MSA)
Cite as Authors (Year) Title. American Mineralogist, in press.
DOI: https://doi.org/10.2138/am-2019-6925

Blundy, J., Cashman, K., and Humphreys, M. (2006) Magma heating by decompression-driven crystallization beneath andesite volcanoes. Nature, 443, 76–80.

Bowen, N.L. (1915) The crystallization of haplobasaltic, haplodioritic, and related magmas. American Journal of Science, 40, 161–185.

Brown, M. (1994) The generation, segregation, ascent and emplacement of granite magma. Earth Science Reviews, 36, 83–130.

Burnham, C.W., and Davis, N.F. (1971) The role of H_2O in silicate melts; I, P-V-T relations in the system $NaAlSi_3O_8$-H_2O to 10 kilobars and 1000 degrees C. American Journal of Science, 270, 54–79.

Burnham, C.W., and Davis, N.F. (1974) The role of H_2O in silicate melts; II, Thermodynamic and phase relations in the system $NaAlSi_3O_8$-H2O to 10 kilobars, 700 degrees to 1100 degrees C. American Journal of Science, 274, 902–940.

Burnham, C.W., Holloway, J.R., and Davis, N.F. (1969) Thermodynamic properties of water to 1,000 degrees C and 10,000 bars. Special Paper 96, Geological Society of America.

Cann, J.R. (1970) Upward movement of granitic magma. Geological Magazine, 107, 335–340.

Clemens, J.D. (1984) Water contents of silicic to intermediate magmas. Lithos, 17, 273–287.

Clemens, J.D., and Mawer, C.K. (1992) Granitic magma transport by fracture propagation. Tectonophysics, 204, 339–360.

Clemens, J.D., and Wall, V.J. (1981) Origin and crystallization of some peraluminous (S-type) granitic magmas. Canadian Mineralogist, 19, 111–131.

Collins, W.J., Huang, H.Q., and Jiang, X. (2016) Water-fluxed crustal melting produces Cordilleran batholiths. Geology, 44, 143–146.

Daly, R.A. (1914) Igneous rocks and their origin, 563 p. McGraw-Hill, New York.

Always consult and cite the final, published document. See http:/www.minsocam.org or GeoscienceWorld

This is a preprint, the final version is subject to change, of the American Mineralogist (MSA)
Cite as Authors (Year) Title. American Mineralogist, in press.
DOI: https://doi.org/10.2138/am-2019-6925

Ganguly, J. (2005) Adiabatic decompression and melting of mantle rocks: An irreversible thermodynamic analysis. Geophysical Research Letters, 32, 1–4.

Giordano, D., Russell, J.K., and Dingwell, D.B. (2008) Viscosity of magmatic liquids: A model. Earth and Planetary Science Letters, 271, 123–134.

Glazner, A.F. (2007) Thermal limitations on incorporation of wall rock into magma. Geology, 35, 319–322.

Glazner, A.F., Coleman, D.S., and Mills, R.D. (2015) The volcanic-plutonic connection. In C. Breitkreuz and S. Rocchi, Eds., Physical Geology of Shallow Magmatic Systems: Dykes, Sills, and Laccoliths, p. 1-22. Springer International Publishing, New York.

Hamilton, W., and Myers, W.B. (1967) The nature of batholiths. U. S. Geological Survey Professional Paper, 554–C, 30 p.

Harris, P.G., Kennedy, W.Q., and Scarfe, C.M. (1970) Volcanism versus plutonism - the effect of chemical composition. In G. Newall and N. Rast, Eds., Mechanism of Igneous Intrusion, pp. 187–200. Liverpool Geological Society, Liverpool.

Jagoutz, O., and Kelemen, P.B. (2015) Role of arc processes in the formation of continental crust. Annual Review of Earth and Planetary Sciences, 43, 363–404.

Johannes, W., and Holtz, F. (1996) Petrogenesis and experimental petrology of granitic rocks, 335 p. Springer, New York.

Lange, R.L., and Carmichael, I.S.E. (1990) Thermodynamic properties of silicate liquids with emphasis on density, thermal expansion and compressibility. In J. Nicholls and J.K. Russell, Eds., Reviews in Mineralogy and Geochemistry Vol. 24, pp. 25–64. Mineralogical Society of America, Washington, D. C.

Lewis, G.N., Randall, M., Pitzer, K.S., and Brewer, L. (1961) Thermodynamics, Second Edition, 723 p. McGraw-Hill, New York.

Always consult and cite the final, published document. See http:/www.minsocam.org or GeoscienceWorld

This is a preprint, the final version is subject to change, of the American Mineralogist (MSA)
Cite as Authors (Year) Title. American Mineralogist, in press.
DOI: https://doi.org/10.2138/am-2019-6925

Mader, H.M., Llewellin, E.W., and Mueller, S.P. (2013) The rheology of two-phase magmas: A review and analysis. Journal of Volcanology and Geothermal Research, 257, 135–158.

McKenzie, D.P., and Bickle, M.J. (1988) The volume and composition of melt generated by extension of the lithosphere. Journal of Petrology, 29, 625–679.

Mercer, C.N., Hofstra, A.H., Todorov, T.I., Roberge, J., Burgisser, A., Adams, D.T., and Cosca, M. (2015) Pre-eruptive conditions of the Hideaway Park topaz rhyolite: insights into metal source and evolution of magma parental to the Henderson porphyry molybdenum deposit, Colorado. Journal of Petrology, 56, 645–679.

Miller, C.F., and Wark, D.A. (2008) Supervolcanoes and their explosive supereruptions. Elements, 4, 11–15.

Müller, A., Kerkhof, A.M. Van Den, Behr, H.J., Kronz, A., Koch-Müller, M. (2010) The evolution of late Hercynian granites and rhyolites documented by quartz – a review. Earth and Environmental Science Transactions of the Royal Society of Edinburgh, 100, 185–204.

Myers, J.S. (1975) Cauldron subsidence and fluidization: mechanisms of intrusion of the Coastal Batholith of Peru into its own volcanic ejecta. Geological Society of America Bulletin, 86, 1209–1220.

Patiño-Douce, A.E., and Beard, J.S. (1995) Dehydration-melting of biotite gneiss and quartz amphibolite from 3 to 15 kbar. Journal of Petrology, 36, 707–738.

Petford, N., Cruden, A.R., McCaffrey, K.J.W., and Vigneresse, J.-L. (2000) Granite magma formation, transport and emplacement in the Earth's crust. Nature, 408, 669–673.

Pinkerton, H., and Stevenson, R.J. (1992) Methods of determining the rheological properties of magma at sub-liquidus temperatures. Journal of Volcanology and Geothermal Research, 53, 47–66.

Always consult and cite the final, published document. See http:/www.minsocam.org or GeoscienceWorld

This is a preprint, the final version is subject to change, of the American Mineralogist (MSA)
Cite as Authors (Year) Title. American Mineralogist, in press.
DOI: https://doi.org/10.2138/am-2019-6925

Pruppacher, H.R., and Klett, J.D. (2010) Cooling of moist air. In J.D. Klett, Ed., Microphysics of clouds and precipitation, p. 485-501. Springer, Dordrecht ; New York.

Ramberg, H. (1971) Temperature changes associated with adiabatic decompression in geological processes. Nature, 234, 539–540.

Robie, R.A., Hemingway, B.S., and Fisher, J.R. (1978) Thermodynamic properties of minerals and related substances at 298.15 K and 1 bar (10^5 Pascals) pressure and at higher temperatures. Bulletin of the United States Geological Survey 1452, 456 p.

Rosera, J.M., Coleman, D.S., and Stein, H.J. (2013) Re-evaluating genetic models for porphyry Mo mineralization at Questa, New Mexico: Implications for ore deposition following silicic ignimbrite eruption. Geochemistry, Geophysics, Geosystems, 14, 787–805.

Rudnick, R.L., and Gao, S. (2013) Composition of the Continental Crust. In Treatise on Geochemistry: Second Edition Vol. 4, pp. 1–51. Elsevier Ltd.

Sato, H. (2005) Viscosity measurement of subliquidus magmas; 1707 basalt of Fuji Volcano. Journal of Mineralogical and Petrological Sciences, 100, 133–142.

Schoene, B., Schaltegger, U., Brack, P., Latkoczy, C., Stracke, A., and Günther, D. (2012) Rates of magma differentiation and emplacement in a ballooning pluton recorded by U-Pb TIMS-TEA, Adamello batholith, Italy. Earth and Planetary Science Letters, 355-356, 162–173.

Shane, P., Nairn, I.A., Smith, V.C., Darragh, M., Beggs, K., and Cole, J.W. (2008) Silicic recharge of multiple rhyolite magmas by basaltic intrusion during the 22.6 ka Okareka Eruption Episode, New Zealand. Lithos, 103, 527–549.

Singer, B.S., Costa, F., Herrin, J.S., Hildreth, W., and Fierstein, J. (2016) The timing of compositionally-zoned magma reservoirs and mafic “priming” weeks before the 1912 Novarupta-Katmai rhyolite eruption. Earth and Planetary Science Letters, 451, 125–137.

Always consult and cite the final, published document. See http:/www.minsocam.org or GeoscienceWorld

This is a preprint, the final version is subject to change, of the American Mineralogist (MSA)
Cite as Authors (Year) Title. American Mineralogist, in press.
DOI: https://doi.org/10.2138/am-2019-6925

346 Singh, S., Kumar, R., Barley, M.E., and Jain, A.K. (2007) SHRIMP U-Pb ages and depth of
347 emplacement of Ladakh Batholith, Eastern Ladakh, India. Journal of Asian Earth Sciences,
348 30, 490–503.
349 Sisson, T.W., Ratajeski, K., Hankins, W.B., and Glazner, A.F. (2005) Voluminous granitic
350 magmas from common basaltic sources. Contributions to Mineralogy and Petrology, 148,
351 635–661.
352 Thomas, J.B., and Watson, E.B. (2012) Application of the Ti-in-quartz thermobarometer to
353 rutile-free systems. Reply to: a comment on: 'TitaniQ under pressure: the effect of pressure
354 and temperature on the solubility of Ti in quartz' by Thomas et al. Contributions to
355 Mineralogy and Petrology, 164, 369–374.
356 Tribaudino, M., Angel, R.J., Cámara, F., Nestola, F., Pasqual, D., and Margiolaki, I. (2010)
357 Thermal expansion of plagioclase feldspars. Contributions to Mineralogy and Petrology,
358 160, 899–908.
359 Tuttle, O.F., and Bowen, N.L. (1958) Origin of granite in the light of experimental studies in the
360 system $NaAlSi_3O_8$-$KAlSi_3O_8$-SiO_2-H_2O. Geological Society of America Memoir, 74, 153.
361 Ussler, W., and Glazner, A.F. (1992) Graphical analysis of enthalpy-composition relationships in
362 mixed magmas. Journal of Volcanology and Geothermal Research, 51, 23–40.
363 Waldbaum, D.R. (1971) Temperature changes associated with adiabatic decompression in
364 geological processes. Nature, 232, 545–547.
365 Wark, D.A., Hildreth, W., Spear, F.S., Cherniak, D.J., and Watson, E.B. (2007) Pre-eruption
366 recharge of the Bishop magma system. Geology, 35, 235–238.
367 Waters, L.E., and Lange, R.A. (2017) Why aplites freeze and rhyolites erupt: Controls on the
368 accumulation and eruption of high-SiO_2 (eutectic) melts. Geology, 45, 1019–1022.

Always consult and cite the final, published document. See http:/www.minsocam.org or GeoscienceWorld

This is a preprint, the final version is subject to change, of the American Mineralogist (MSA)
Cite as Authors (Year) Title. American Mineralogist, in press.
DOI: https://doi.org/10.2138/am-2019-6925

Waters, L.E., Andrews, B.J., and Lange, R.A. (2015) Rapid crystallization of plagioclase phenocrysts in silicic melts during fluid-saturated ascent: phase equilibrium and decompression experiments. Journal of Petrology, 56, 981–1006.

Always consult and cite the final, published document. See http:/www.minsocam.org or GeoscienceWorld

This is a preprint, the final version is subject to change, of the American Mineralogist (MSA)
Cite as Authors (Year) Title. American Mineralogist, in press.
DOI: https://doi.org/10.2138/am-2019-6925

Figure 1

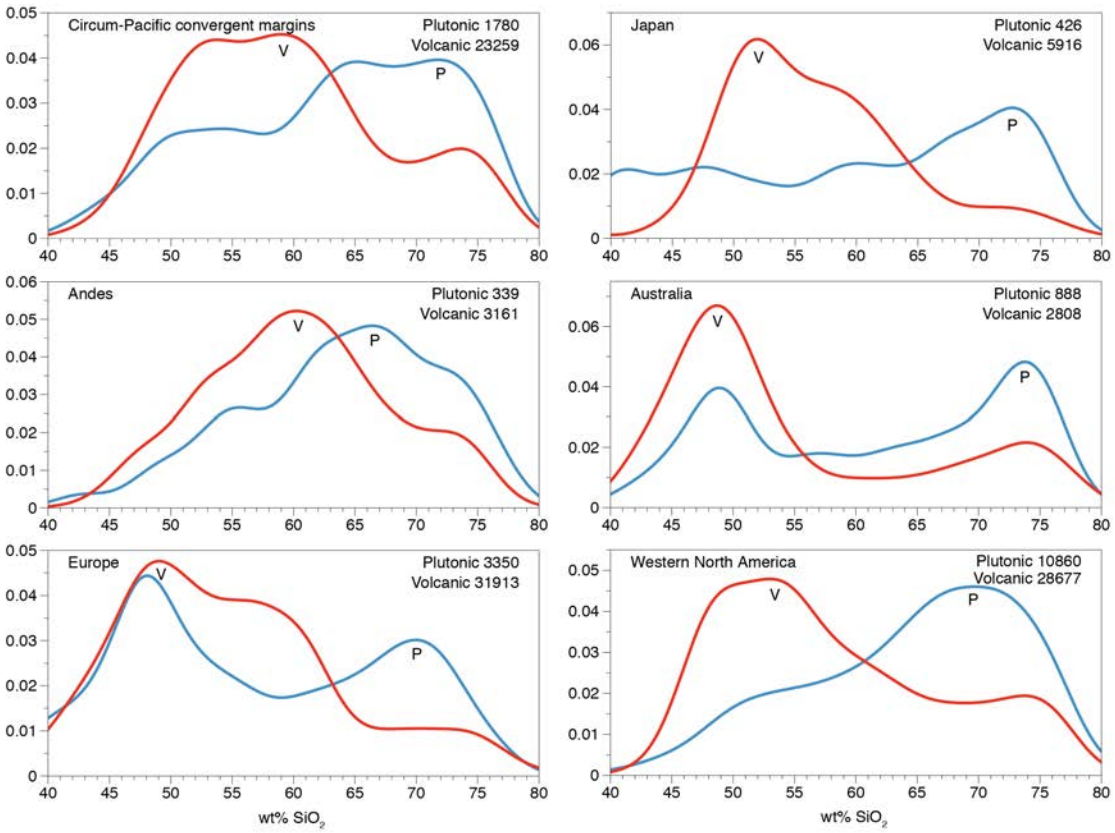

Figure 1. Distributions of silica contents of volcanic (V) and plutonic (P) rocks from various continental geologic provinces: Circum-Pacific convergent margins (dataset of (Glazner et al. 2015)); Japan (Earthchem); Andes, Cenozoic and Mesozoic (Earthchem); Australia (GEOROC); Europe (Earthchem); Western North America, Cenozoic and Mesozoic (NAVDAT). Curves are kernel density plots using Gaussian kernels with a standard deviation of 2 wt%; number of analyses in each group is indicated.

Always consult and cite the final, published document. See http:/www.minsocam.org or GeoscienceWorld

This is a preprint, the final version is subject to change, of the American Mineralogist (MSA)
Cite as Authors (Year) Title. American Mineralogist, in press.
DOI: https://doi.org/10.2138/am-2019-6925

Figure 2

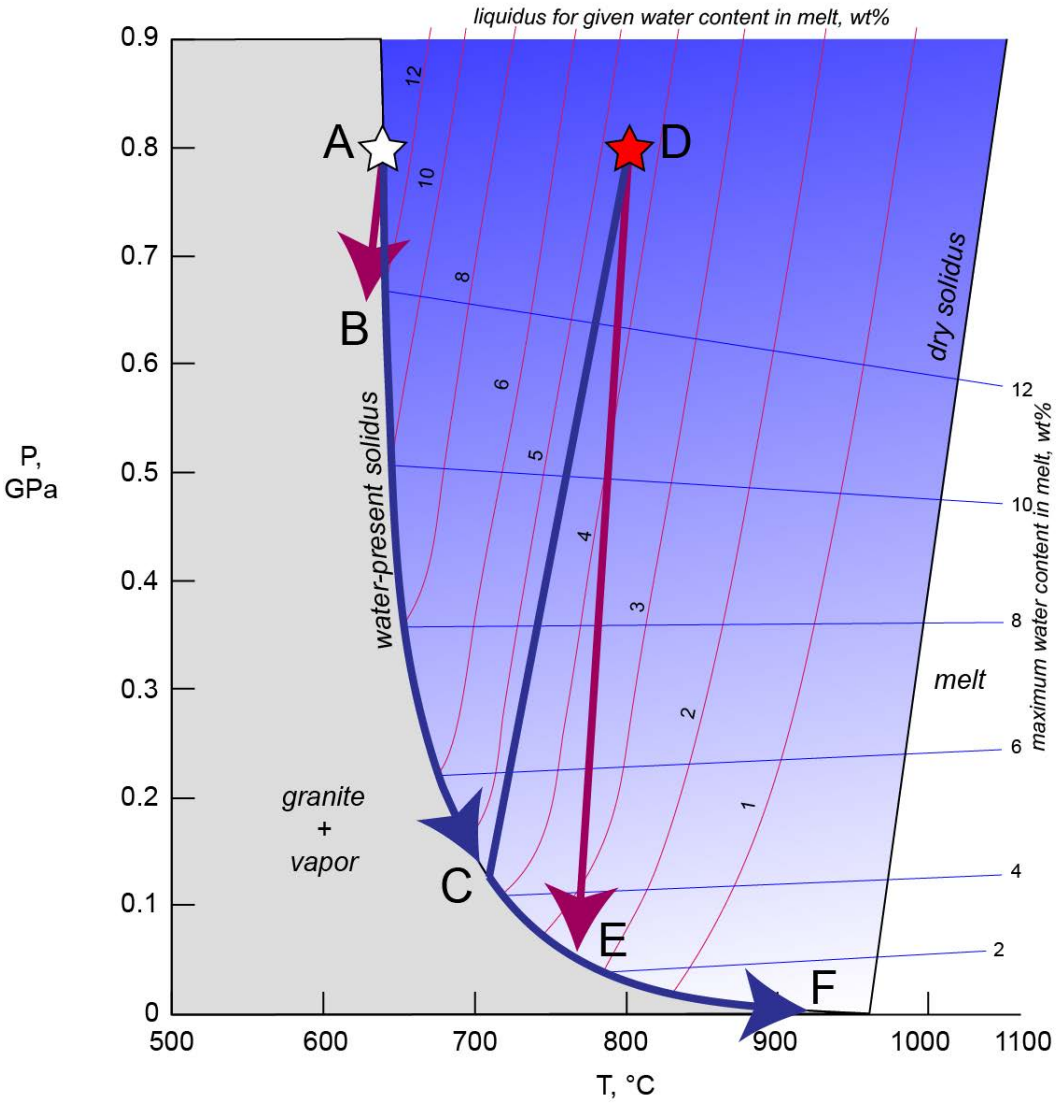

Figure 2. Pressure-temperature diagram for melting of granite in the presence of water (Johannes and Holtz 1996). Owing to the negative slope of the water-present solidus, it has long been assumed that ascent of magma from the solidus (path A-B) cannot occur because such a magma will freeze upon leaving the solidus (Tuttle and Bowen 1958; Cann 1970; Harris et al. 1970). Shallow emplacement of granites is generally attributed to generation of magma at temperatures well above the solidus by dehydration melting, followed by ascent to the solidus, where they freeze (path D-E). However, treating ascent as an adiabatic, isentropic process indicates that magmas generated on or reaching the solidus will follow it to shallow depth and possibly the surface (paths A-C-E-F and D-C-F), partially crystallizing and exsolving water-rich vapor along

Always consult and cite the final, published document. See http:/www.minsocam.org or GeoscienceWorld

This is a preprint, the final version is subject to change, of the American Mineralogist (MSA)
Cite as Authors (Year) Title. American Mineralogist, in press.
DOI: https://doi.org/10.2138/am-2019-6925

the way. Gently sloping blue curves give maximum water content in melt in weight percent, and steeply sloping red curves give the liquidus for the given water contents.

Figure 3

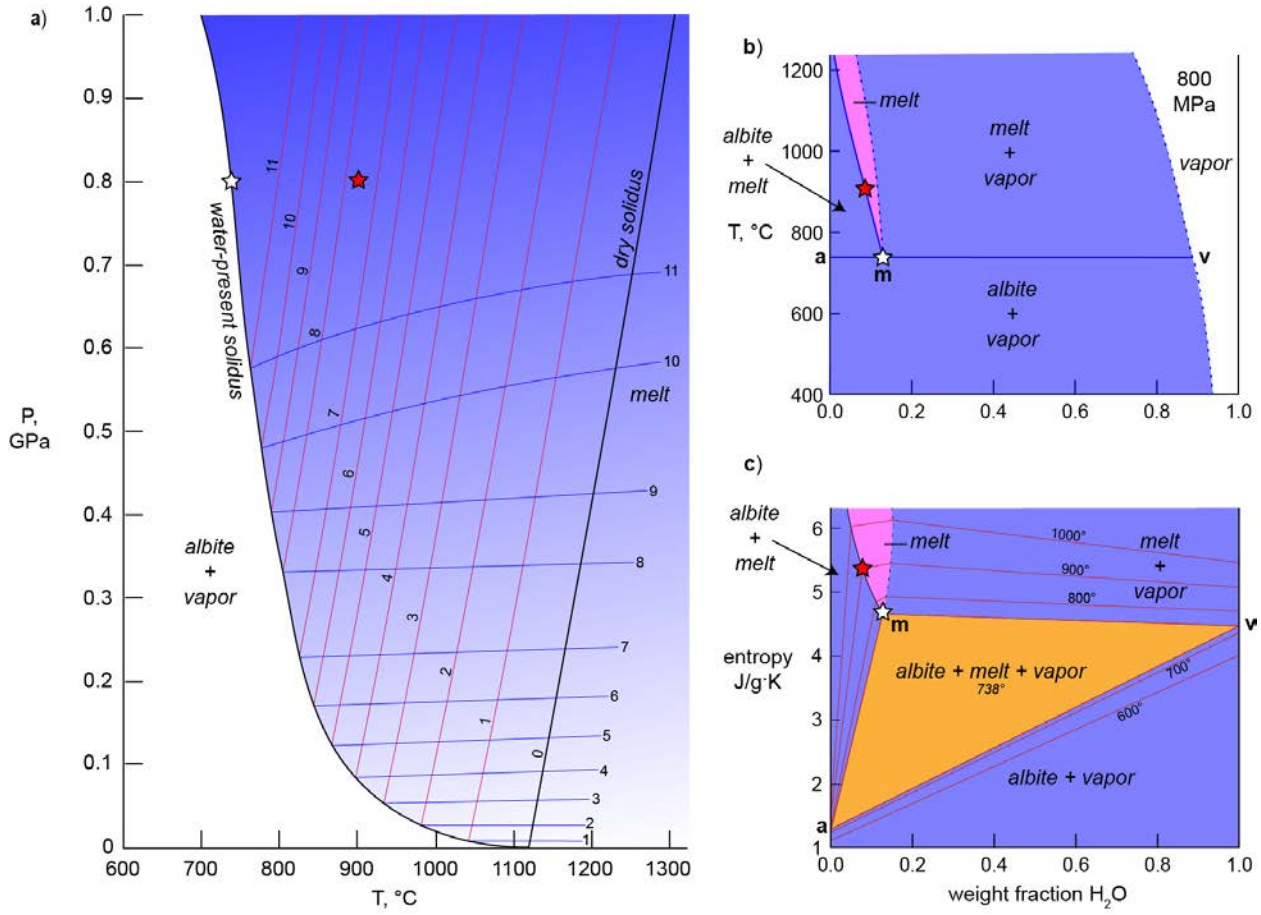

Figure 3. Pressure-temperature-entropy relations in the system albite-H_2O. a) P-T projection from (Burnham and Davis 1974). Gently sloping blue curves give maximum water content in melt in weight percent, and steeply sloping red curves give the liquidus for the given water contents. White star in all panels represents melt generated at the water-present solidus, and red star represents a water-undersaturated melt generated by dehydration melting at 900 °C. b) Isobaric section at P = 800 MPa; dashed boundaries of melt+vapor and dashed vapor side of albite+vapor are not well determined. c) Isobaric section, as in panel B, recast as specific entropy (s) vs. composition, contoured for T. The albite+melt+vapor invariant point has expanded into a three-phase triangle. Vapor composition is idealized as pure H_2O, and dashed melt+vapor boundary is schematic.

Always consult and cite the final, published document. See http:/www.minsocam.org or GeoscienceWorld

This is a preprint, the final version is subject to change, of the American Mineralogist (MSA)
Cite as Authors (Year) Title. American Mineralogist, in press.
DOI: https://doi.org/10.2138/am-2019-6925

Figure 4

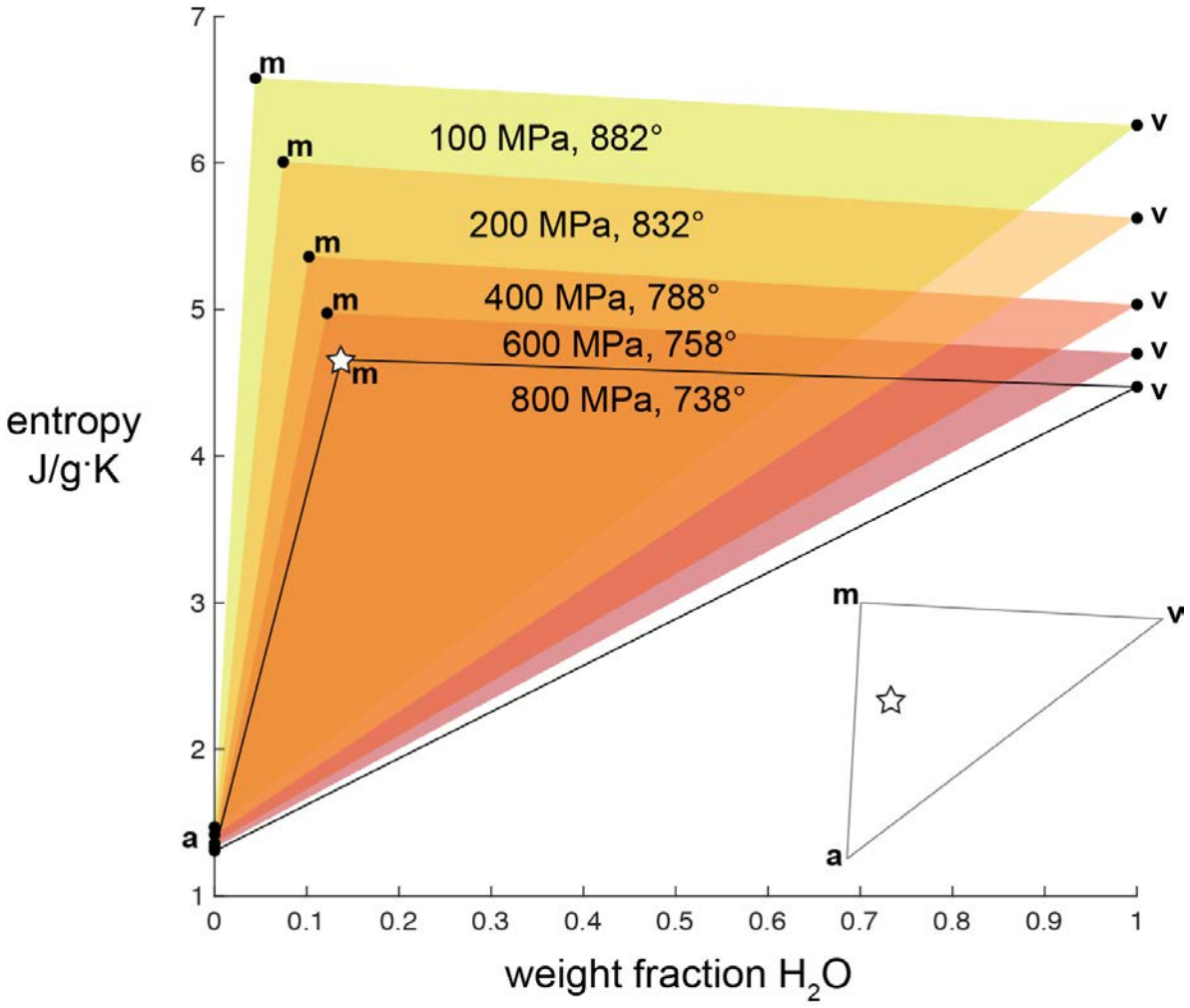

407

408 **Figure 4**. Entropy triangles at the solidus as a function of pressure. Triangles connect albite
409 crystals (**a**), hydrous melt (**m**), and water-rich vapor (**v**), all in equilibrium along the water-
410 present solidus at indicated pressures (MPa) and temperatures (°C). If hydrous melt at 800 MPa
411 (star) rises adiabatically and reversibly, then the entropy and bulk composition of the system
412 remain at the star and the proportions of the three phases at lower pressures can be determined
413 using the lever rule; e.g., at 200 MPa the system will consist of 29 wt% albite, 62 wt% melt, and
414 9 wt% vapor at 832 °C. As an example, inset shows the 100 MPa entropy triangle along with the
415 800 MPa melt composition, showing the proportions that the 800 MPa melt will evolve to upon
416 adiabatic ascent to 100 MPa. The melt partially crystallizes and exsolves vapor as it rises to
417 shallower depth and lower pressure.

Always consult and cite the final, published document. See http:/www.minsocam.org or GeoscienceWorld

This is a preprint, the final version is subject to change, of the American Mineralogist (MSA)
Cite as Authors (Year) Title. American Mineralogist, in press.
DOI: https://doi.org/10.2138/am-2019-6925

Figure 5

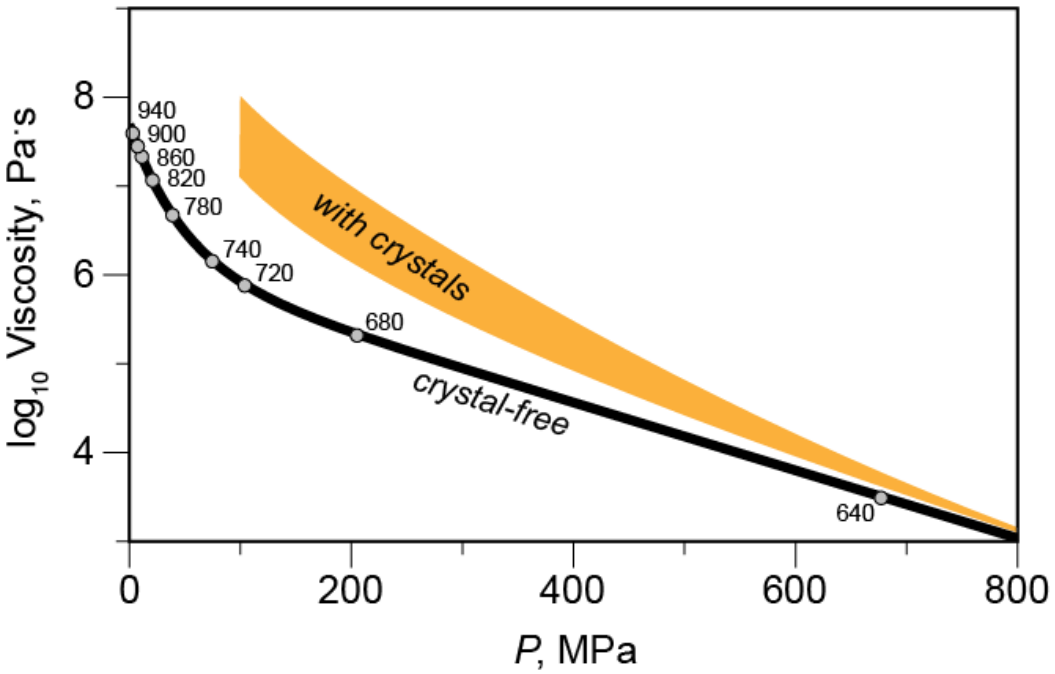

Figure 5. Viscosity of melt in the granite system along the water-present solidus. Calculated (Giordano et al., 2008) viscosity of water-saturated melt rises exponentially as pressure drops from 800 to 200 MPa, and then super-exponentially at lower pressures. Values along the curve give corresponding temperatures along solidus. Band at higher viscosity show the effects of adding in the crystal proportions indicated in the albite-H_2O system down to 100 MPa as a rough guide to how crystallization adds to the viscosity; range of curves represents two different models (Sato 2005; Mader et al. 2013).

Always consult and cite the final, published document. See http:/www.minsocam.org or GeoscienceWorld

Figure 6

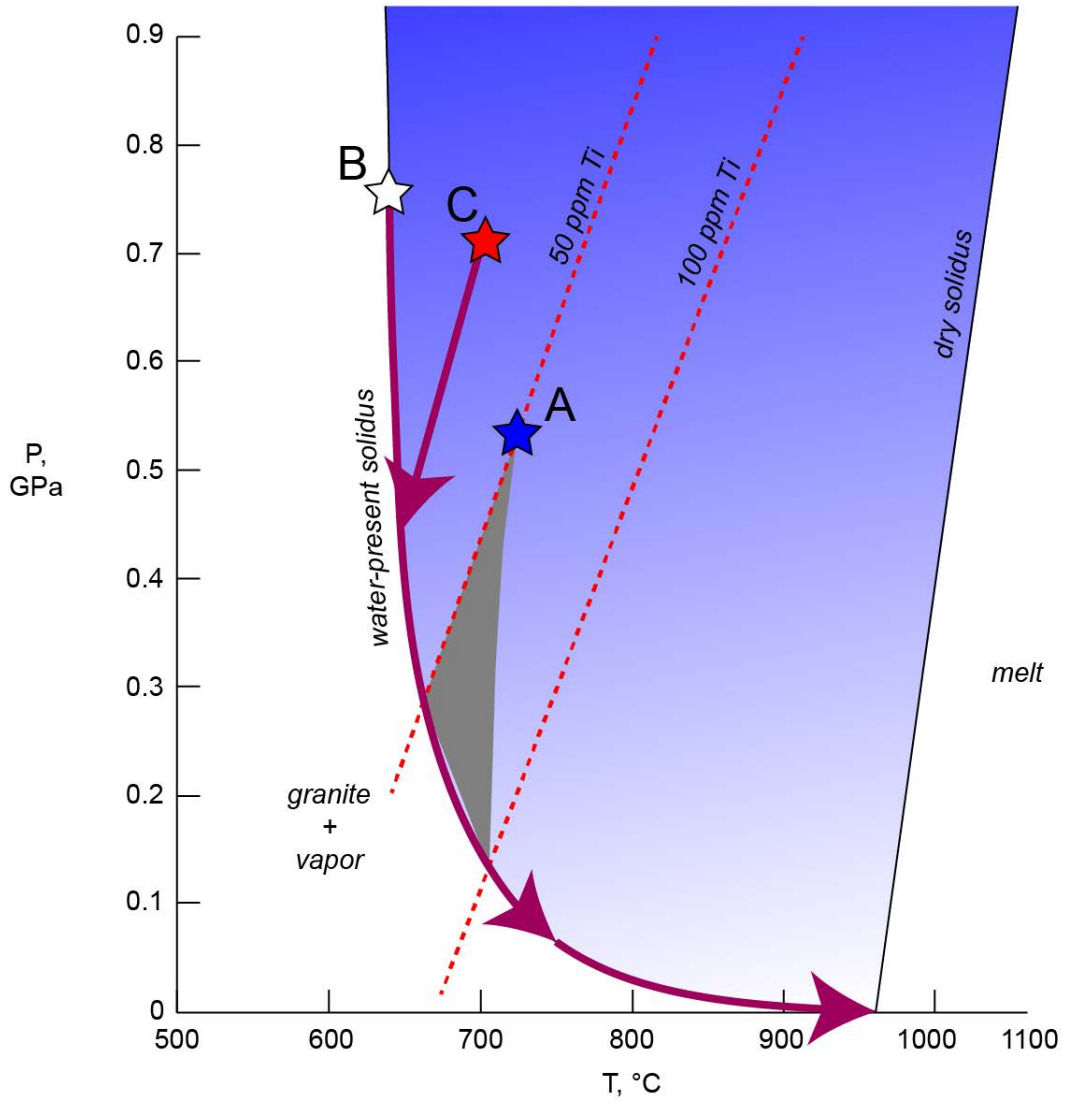

Figure 6. Decompression heating and Ti-in-quartz thermobarometry. Quartz crystals in many rhyolites and granites show rimward increases in Ti content, typically from ~50 ppm to ~100 ppm. These increases are generally interpreted as a sign of heating by magma recharge (Wark et al. 2007), but (Thomas and Watson 2012) proposed that near-isothermal ascent of water-undersaturated magma (A) from the 50 ppm isopleth to the 100 ppm isopleth (paths within gray triangle) could produce Ti-rich rims by decompression. I propose that rising silicic magma generated under either water-saturated (B) or undersaturated (C) conditions will follow the solidus to lower pressure and higher temperature, leading to crystal growth, heating, and the observed rimward increases in Ti.

Always consult and cite the final, published document. See http:/www.minsocam.org or GeoscienceWorld